

# Exploring Context Modeling Techniques on the Spatiotemporal Crowd Flow Prediction

Liyue Chen  
chenliyue2019@gmail.com  
Peking University  
Beijing, P.R.China

Leye Wang\*  
leyewang@pku.edu.cn  
Peking University  
Beijing, P.R.China

## ABSTRACT

In the big data and AI era, context is widely exploited as extra information which makes it easier to learn a more complex pattern in machine learning systems. However, most of the existing related studies seldom take context into account. The difficulty lies in the unknown generalization ability of both context and its modeling techniques across different scenarios. To fill the above gaps, we conduct a large-scale analytical and empirical study on the spatiotemporal crowd prediction (STCFP) problem that is a widely-studied and hot research topic. We mainly make three efforts: (i) we develop new taxonomy about both context features and context modeling techniques based on extensive investigations in prevailing STCFP research; (ii) we conduct extensive experiments on seven datasets with hundreds of millions of records to quantitatively evaluate the generalization ability of both distinct context features and context modeling techniques; (iii) we summarize some guidelines for researchers to conveniently utilize context in diverse applications.

### ACM Reference Format:

Liyue Chen and Leye Wang. 2021. Exploring Context Modeling Techniques on the Spatiotemporal Crowd Flow Prediction. In *Singapore '21: ACM Knowledge Discovery and Data Mining (KDD), April 14-18, 2021, Singapore*. ACM, New York, NY, USA, 11 pages. <https://doi.org/10.1145/1122445.1122456>

## 1 INTRODUCTION

Context has proved useful as feature inputs for a wide variety of tasks such as weather data for bike-sharing demand forecast [11]. In general, context is any information that can be used to characterize the situation of an entity, where an entity can be a person, place, or physical or computational object [1]. Understanding context is not trivial as it can provide extra useful information that can be fed to machine learning systems and help in learning specific patterns.

However, previous works have focused on the selective context in specific applications, and the generalization ability of context is still unknown: for example, the distinctive context in some scenarios may not work in other scenarios. More specifically, choosing

appropriate context from a wide variety of contexts for their application is a significant issue.

This question is especially difficult because the frontier studies on leveraging the context features still suffer from the following pitfalls:

- *Lacking a taxonomy of context features.* There are many types of context features and most studies only consider a small part of them. A comprehensive taxonomy is desired.
- *Confusing modeling techniques.* Previous studies propose diverse context modeling techniques that may be useful in their settings. But for the new-coming researchers, it is usually confusing to determine an appropriate modeling technique that suits their application scenarios.
- *The generalization ability of different context is yet unknown.* Due to the diversity of context features, selecting the appropriate and beneficial context is hard. To the best of our knowledge, no previous study has thoroughly compared the capabilities of diverse context features with different modeling techniques in a variety of real-life problems.

Though the context applies to many fields, in this paper, we focus on the Spatiotemporal Crowd Flow Prediction (STCFP) problem for two reasons. First, STCFP is a classic and well-studied problem including traffic flow prediction [7, 18], bikesharing demand prediction [3, 11], ridesharing demand prediction [6, 9, 27] and the charging demand of electric vehicles [2]. So we can make full use of these newest approaches and models. Second, there are lots of open-access datasets in this field such as the bikesharing dataset<sup>1</sup>, which makes it feasible to the further study.

In STCFP studies, researchers usually consider spatial and temporal dependencies and discover many kinds of spatiotemporal knowledge. Temporal dependency denotes the relation between future flow and past crowd flow, while spatial dependency mainly considers the relation between different stations in different geographic locations. Meanwhile, context knowledge also plays a key role. Take weather context as an example, rising temperatures will promote the use of bike-sharing [11] and heavy rains will lessen bike-sharing and online ride-hailing usage [8]. Besides, pioneering studies try to design some techniques to make full use of context information and propose different context modeling techniques such as *Embedding* [3], *Multiple Embedding Layers* [14], *Late Adding Fusion* [28], *LSTM* [9] and *Gating* [29].

Spatiotemporal knowledge and context knowledge both provide useful information in real STCFP problems. While prior studies have proposed many dedicated techniques to model spatiotemporal knowledge in better ways (e.g. attention mechanism [12] and graph

\*Corresponding author.

Permission to make digital or hard copies of all or part of this work for personal or classroom use is granted without fee provided that copies are not made or distributed for profit or commercial advantage and that copies bear this notice and the full citation on the first page. Copyrights for components of this work owned by others than ACM must be honored. Abstracting with credit is permitted. To copy otherwise, or republish, to post on servers or to redistribute to lists, requires prior specific permission and/or a fee. Request permissions from [permissions@acm.org](mailto:permissions@acm.org).

*KDD '21, April 14-18, 2021, Singapore*

© 2021 Association for Computing Machinery.  
ACM ISBN 978-1-4503-XXXX-X/18/06...\$15.00  
<https://doi.org/10.1145/1122445.1122456>

<sup>1</sup><https://www.citibikenyc.com/system-data>

convolution network [3, 6]), context features are usually used casually without careful design and evaluation. For instance, previous STCFP studies [9, 14, 28, 29] have proposed several kinds of techniques to model diverse types of context features, but they all do not further evaluate the effectiveness of chosen context features and modeling techniques.

To sum up, in this paper, we aim to explore the generalization of context as well as its modeling techniques in a variety of STCFP scenarios. To this end, we conduct a large-scale analytical and experimental empirical study. Particularly, we try to give some design guidelines for future research and make the following contributions:

- We investigate the context features which are especially general in the frontier STCFP studies, and the context is further classified into weather, holiday, temporal position, and POI.
- We elaborate on existing context modeling techniques and develop a taxonomy. Based on our taxonomy, we analyze existing context modeling techniques, and more importantly, discover new ones that are never studied in literature (e.g. *LSTM-Gating* in Sec 4.2).
- We conduct large-scale experiments on seven real-world datasets of four STCFP scenarios. Based on our experiments, we evaluate the capability of diverse modeling techniques and the generalization ability of different types of context. By analyzing the experiment results, we summarize some guidelines about choosing context features and modeling techniques.

## 2 PRELIMINARY

We first define several key concepts and then formulate the Spatiotemporal Crowd Flow Prediction problem:

**Definition 1** *Crowd Flow*: In spite of diverse application scenarios and different prediction tasks, we call all the predict target as crowd flow if they are related to people’s mobility (e.g., taxi demand and metro station flow). Suppose that there are  $n$  locations and in each location it has a historical series of crowd flow records from time slot 1 to the current slot  $k$ . The crowd flow in each location at time  $i$  can be denoted as:

$$F^i = \{f_1^i, f_2^i, \dots, f_n^i\} \quad (1)$$

**Definition 2** *Context*: Suppose that there are  $m$  different kinds of context information and the context features at time  $i$  are denoted as:

$$E^i = \{e_1^i, e_2^i, \dots, e_m^i\} \quad (2)$$

Note that each element in  $E^i$  has  $n$  dimensions representing  $n$  locations.

**Definition 3** *Latent Representation of Spatiotemporal features*: The latent representation of spatiotemporal features are the outputs of spatiotemporal modeling units which can both capture spatial and temporal correlation (e.g. DCRNN[10]). For the convenience of description, the latent representation after spatiotemporal aggregation units in highest layers at time  $i$  are denoted as  $ST^i$ . The latent representation of spatiotemporal features can be denoted as:

$$ST = \{ST^0, ST^1, \dots, ST^k\} \quad (3)$$

**Table 1: The context in STCFP application.**

Context	Description
<b>Weather</b>	
Temperature	average surface temperature over a period of time
Pressure	atmospheric pressure at sea level
Humidity	relative concentration of water vapor present in the air
Visibility	the distance that an object or light can be discerned
Wind Speed	wind speed at the moment of measurement
Wind Degree	the direction that wind is blowing
Clouds	the ratio of cloud obscuring the view of the sky
Weather State	weather conditions, such as fog/snow/clear/rain
<b>Holiday</b>	
Workday	working day
Dayoff	national statutory holiday
<b>Temporal Position</b>	
DayofWeek	day indicator in one week
HourofDay	hour indicator in one day
<b>POI</b>	
POI density	POI density of different categories

**Problem** For each location, given the historical crowd flow observations  $\mathcal{F} = \{F^0, F^1, \dots, F^k\}$  and context  $\mathcal{E} = \{E^0, E^1, \dots, E^k\}$ , predict  $F^{k+1}$ . And the optimization goal is to minimize the prediction error:

$$\min error(\hat{F}^{k+1}, F^{k+1}) \quad (4)$$

where  $\hat{F}^{k+1}$  is the predicted flow at time slot  $k + 1$ , and  $F^{k+1}$  is the ground truth; the error function can be RMSE (root mean square error). We need to learn a function  $g(\cdot)$  that map historical crowd flow and context features into future crowd flows:

$$\hat{F}^{k+1} = g(\mathcal{F}, \mathcal{E}) \quad (5)$$

STCFP problem is an abstraction of many real-world applications and thus has broad application prospects. There are varieties of application scenarios based on STCFP such as metro human flow [20], electrical vehicle charging usage [2], ridesharing demand prediction [6] and bikesharing demand prediction [3].

## 3 ANALYTICAL STUDIES ON CONTEXT FEATURES

In this section, we conduct analytical studies that mainly focus on context features. We first revisit context features mentioned in recent STCFP studies and give a taxonomy of context (listed in Table 1). Moreover, we introduce the context data preprocessing methods.

### 3.1 Taxonomy of Context Features

**3.1.1 Weather.** In general, weather context such as temperature, humidity, wind speed and weather conditions (and etc.) refers to short-term changes in the atmosphere<sup>2</sup> and can indeed influence crowd flow [8, 11, 21]. For instance, rising temperatures will increase the use of bikesharing [11]. Heavy rains and strong winds will reduce the use of bikesharing and online ride-hailing [8]. The

<sup>2</sup><https://www.ncei.noaa.gov/news/weather-vs-climate>

crowd flow in different STCFP application scenarios may be affected by different kinds of weather context. To show the difference, we give weather context usage statistics in Table 2. It is not surprising that temperature and weather state are the most important considerations because when a person is out, he will observe the weather condition and temperature to decide whether he goes out or not.

**3.1.2 Holiday.** In the real world, the crowd flow daily pattern is closely related to holidays. There is an obvious migration flow from urban residential areas to business areas during the workday, but this pattern is not so clear on holiday. Hoang’s research also reveals that the subway traffic pattern on weekends is obviously different from that on weekdays [8].

**3.1.3 Temporal Position.** Crowd flow patterns are different for each day in a week. As an illustration, the crowd flow on Friday night is usually higher than that on Thursday night. The hourly crowd flow patterns in one day may also be different, for example, the peak traffic in the morning and evening is significantly higher than the traffic in off-peak hours. This phenomenon reveals that the crowd flow patterns at different temporal periods are dissimilar. We use two hard-coded indicators to record temporal position features of crowd flow:

- *HourofDay* indicates where the current time is in one day (what time it is), and its value range is between 0 and 23 (representing 0 o’clock 23 o’clock). A more reasonable approach is to treat *HourofDay* as discrete features, and then transform them by one-hot encoding.
- *DayofWeek* indicates where the current time is in one week (which day it is). The value range of *DayofWeek* is between Monday and Sunday and it can be transformed by one-hot encoding similarly [14].

**3.1.4 Point of Interest.** Point of Interest(POI) are specific point locations that someone may find useful or interesting including residential areas, business areas, and tourist attractions in the city. POI context can greatly improve our understanding of these locations’ traffic patterns[26]. POI context is usually considered as a kind of extra spatial information that helps model spatial correlations. [12, 15].

**3.1.5 Others.** We list the general context that could be applied in almost every STCFP scenario. However, the context is quite diverse for various kinds of specific applications and not limited to the above. When predicting geographical sensors’ time series, researchers also consider using sensor ID as context features[12]. When predicting taxi demand, researchers also take the effects of special events and discount pricing strategy into account [15].

## 3.2 Context Data Preprocessing Methods

Context is often collected by various geographical sensors in meteorological stations, resulting in two types of data: continuous and discrete. The continuous context is with specific numerical value, e.g. temperature( $^{\circ}$ F), humidity(%), and wind speed(m/s). The discrete context is with labels, e.g. weather state (sunny/rainy/...) and holiday (workday/holiday).

Continuous context can be directly fed into the neural network as features. However, discrete contexts like weather state, holiday,

temporal position data, and POI, should be encoded first by some transformation (e.g. one-hot encoding or embedding). For example, *HourofDay* context can be encoded into a one-hot vector of length 24, which represents the index of an hour in the day. The *DayofWeek* context can be encoded into a vector of length 7. For the POI context, researchers count the POI density of different categories as features [15].

However, one-hot encoding may explode the context dimensions which may result in the curse of dimensionality issue. Researchers reduce context feature with large dimensions by manual coding, e.g. categorizing the weather state into good weather (sunny, cloudy) and bad weather (rainy, storm, dusty) [4, 8]. Other researchers use *Embedding* [3, 27] and *PCA (Principal Component Analysis)* methods to achieve this end. We will elaborate on context modeling techniques in the next section.

## 4 ANALYTICAL STUDIES ON CONTEXT MODELING TECHNIQUES

For the convenience of understanding context modeling techniques, we first introduce a flexible and transparent framework named *STMeta* (Figure 1 Block A). Note that backbone *STMeta* network is consist of two main components and can model different types of spatial and temporal dependencies. The first component is spatiotemporal modeling units (e.g. *GCLSTM* [3] and *DCGRU* [10]) which can capture diverse types of spatiotemporal dependencies and the second component is spatiotemporal aggregation units that aggregate different types of spatiotemporal features (e.g. graph attention layer[16] and concatenate). With advanced *STMeta* framework, existing context modeling techniques are classified into **Early Jointly Modeling** (Figure 1 Block B) and **Late Fusion Modeling** (Figure 1 Block C) and the latter can be further considered of a two-stage process.

### 4.1 Early Jointly Modeling

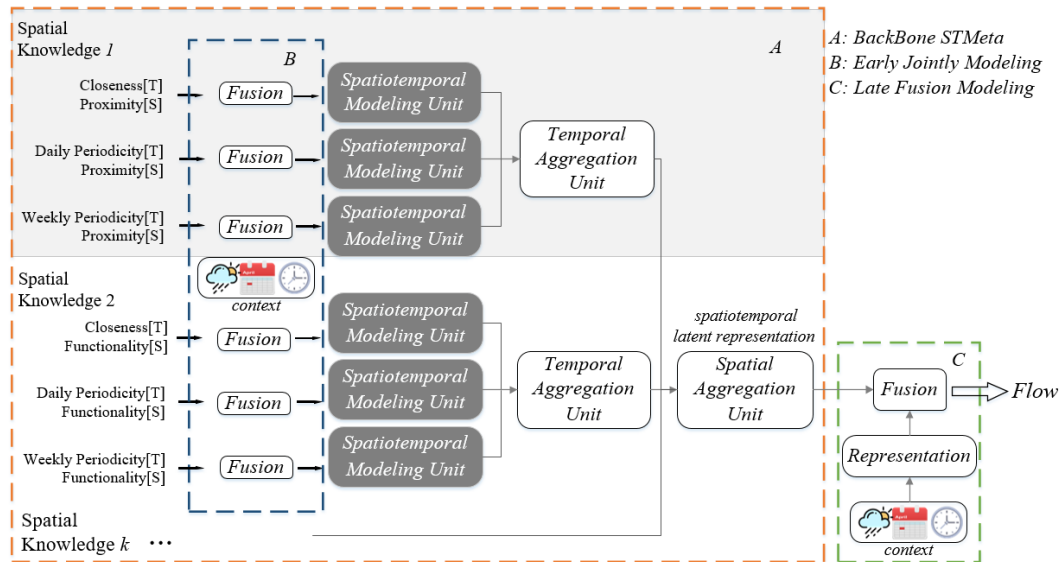
Early jointly Modeling refers to fusing context features with spatiotemporal features before further capturing spatiotemporal dependencies via a neural network (Block B in Figure 1). For example, Lin et al.[13] combine *DayofWeek*, *HourofDay* features and POI (Point of Interest) map with population distribution map by using adding, and then apply ResPlus structure to capture deeper long-spatial dependence. Yao et al. [23, 24] concatenate spatial view (a kind of latent spatial representation) and context feature, then capture temporal dependencies by *LSTM*. We name the above modeling techniques *EarlyAdd* and *EarlyConcat* respectively. However, early fusion modeling is not commonly used in literature because it may bring a higher computational burden. Most studies leverage late fusion modeling, which we elaborate on next.

### 4.2 Late Fusion Modeling

Late Fusion Modeling means fusing context features and other features in the high-level layer of neural network (Figure 1 block C). Remember that  $E^i$  and  $ST^i$  are context features and latent spatiotemporal representation at time  $i$ . The output of late fusing modeling modules can be denoted by  $O$ . We investigate existing studies related to the STCFP problem. For better understanding, we elaborate on these methods in two stages:

**Table 2: Context features and its modeling techniques in STCFP Studies. (T: Temperature; H: Humidity; V: Visibility; WS: Wind Speed; WD: Wind Degree; AQ: Air Quality; S: Weather State)**

	Weather	Holiday	Temporal Position	POI	Modeling Method
<b>Bikesharing</b>					
Li et al. 2015 [11]	T;WS,S				Raw-Concat
Yang et al. 2016 [22]	T;H;V;WS,S		✓		
Chai et al. 2018 [3]	T;WS,S	✓			Emb-Concat
<b>Ridesharing</b>					
Tong et al. 2017 [15]	T;H;WS;WD;AQ;S	✓	✓	✓	Raw-Concat
Ke et al. 2017 [9]	T;H;V;WS,S		✓		LSTM-Add
Wang et al. 2017 [17]	T;AQ;S				MultiEmb-Concat
Zhu et al. 2017 [30]		✓			Raw-Concat
Yao et al. 2018 [24]	T;S	✓			EarlyConcat
<b>Metro Crowd Flow</b>					
Liu et al. 2019 [14]	S		✓		MultiEmb-Concat
<b>Citywide Crowd Flow</b>					
Hoang et al. 2016 [8]	T				Raw-Concat
Zhang et al. 2016 [28]			✓		Raw-Add
Zhang et al. 2017 [27]	T;WS;S	✓			Emb-Add
Zonoozi et al. 2018 [31]			✓		Raw-Add
Zhang et al. 2019 [29]	T;WS;S	✓			Raw-Gating
Yi et al. 2019 [25]			✓		Emb-Add
Chen et al. 2020 [4]	S		✓		EarlyConcat

**Figure 1: Early Jointly Modeling and Late Fusion Modeling modeling techniques based on STMeta backbone network.****Stage 1: Context Representation**

The first stage is to capture the different pattern of context by the following techniques:

- *Raw*. Do not change feature dimensions and preserve original features, yet it may lack the ability to capture more context information.
- *Embedding*. The Embedding technique is widely used in various fields, such as NLP (natural language processing). It can

map high-dimension features to low-dimension features that can represent the similarities of vectors. Many studies use high to low dimension fully-connected layer as embedding layer [3, 27]. For instance, Zhang et al. [27] use two fully-connected layers upon context features  $E^i$ , the first layer can be viewed as an embedding layer.

- *Multiple Embedding*. Different types of context features can be fed into multiple embedding layers [12, 14, 17]. That is

the difference between *Embedding* and *Multiple Embedding*.

$$\mathcal{E}' = \text{Concat}(\text{Emb}(E_1); \text{Emb}(E_2); \dots; \text{Emb}(E_m)) \quad (6)$$

- *LSTM*. Context features are time-varying time-series variables and past context features may have a significant impact on future flow. For example, sudden heavy rain may immediately reduce the crowd flow, but when the rain stops, the crowd flow may be larger than ever. To capture the temporal dependencies of context features, Ke et al. [9] use *LSTM* to capture temporal dependencies of context features.

## Stage 2: Feature Fusion

Stage 2 is to fuse context with other features (usually are spatiotemporal latent representation) and acquire target output. Note that the context feature after **Context Representation** stage can be denoted as  $\mathcal{E}'$  ( $\mathcal{E}' \in \mathcal{R}^{k \times n \times p}$ ),  $k$  is the number of historical record,  $n$  is the number of stations and  $p$  is the dimension of fusion features. Context  $\mathcal{E}'$  can be fused by the following techniques:

- *Concatenate*. *Concatenate* is a general and most commonly used technique which combines different features along features axis. Chai et al. [3] use a fully connected layer as embedding layer to represent context features and then concatenate context features  $\mathcal{E}'$  with spatiotemporal latent representation  $\mathcal{ST}$ . The *Concatenate* formula is:

$$O = \text{Concat}(\mathcal{E}'; \mathcal{ST}) \quad (7)$$

- *Add*. Compared with *Concatenate* fusion method, *Add* doesn't expand the dimension of hidden states and thus has a lower computational cost. The formula of *Add* is:

$$O = W_e \cdot \mathcal{E}' + W_{st} \cdot \mathcal{ST} + b \quad (8)$$

note that  $W_e$ ,  $W_{st}$  and  $b$  are learnable parameters.

- *Gating*. *Gating-mechanism-based* [29] fusion consider context features as the activation function of spatiotemporal features. It first transform the context feature to gating value  $G$  and then use  $G$  to activate spatiotemporal features:

$$G = \sigma(W_e \cdot \mathcal{E}' + b), O = \sigma(G \otimes \mathcal{ST}) \quad (9)$$

where  $W_e$  and  $b$  are learnable parameters, " $\cdot$ " and " $\otimes$ " are the dot product and hadamard product of two vectors. The intuition of *Gating* is that context features are like a switch, the crowd flows would be tremendously changed if activated. Based on this insight, Zhang et al. [29] use *Gating* technique to model context features and their experiment results demonstrate that *Gating* technique can help enhance performance.

It is apparent that there are remaining other variants by combining two stages in **Late Fusion Modeling** branch (e.g. *LSTM-Gating* is consist of *LSTM* and *Gating*), we list existing modeling techniques based on our taxonomy in Table 3.

## 5 EXPERIMENTAL EMPIRICAL STUDIES

### 5.1 Dataset

We conduct experiments on seven city datasets including four scenarios (bikesharing demand, ridesharing demand, metro flow, and electric vehicle charging station usage). The dataset descriptions and statistics are listed in Appendix C and Table C1. Original records

**Table 3: Late Fusion Modeling details which consist of representation and fusion stage. Modeling techniques with "\*" are newly proposed based on our taxonomy.**

Name	Representation	Fusion	Literature
<i>Raw-Concat</i>		Concat	[30]
<i>Raw-Add</i>	Raw	Add	[28, 31]
<i>Raw-Gating</i>		Gating	[29]
<i>Emb-Concat</i>		Concat	[3]
<i>Emb-Add</i>	Embedding	Add	[25, 27]
<i>Emb-Gating*</i>		Gating	-
<i>MultiEmb-Concat</i>		Concat	[12, 14, 17]
<i>MultiEmb-Add*</i>	Multiple Embedding	Add	-
<i>MultiEmb-Gating*</i>		Gating	-
<i>LSTM-Concat*</i>		Concat	
<i>LSTM-Add</i>	<i>LSTM</i>	Add	[9]
<i>LSTM-Gating*</i>		Gating	-

are processed at an interval of 60 minutes and the task is to predict the flow in the next hour.

### 5.2 Experiment Settings

**5.2.1 Data Split.** We split the original data into train-set and test-set at the ratio of 9:1. We use the last 10% duration before the test-set for validation.

**5.2.2 Model Variants.** We implement following variants that are mentioned in Sec 4 based on *STMeta* backbone network:

- **STMeta:** *STMeta* [19] is our backbone network that only considers spatiotemporal dependencies.
- **Early Joint Modeling:** Following the definitions in Sec 4.1, this branch fuses context with spatiotemporal features before the spatiotemporal modeling units. We implement *EarlyConcat* and *EarlyAdd* variants.
- **Late Fusion Modeling:** By combining two stages mentioned in Sec 4.2, we implement twelve variants. For example, the variants whose first stage is *LSTM* and the second stage is *Gating* will be named as *LSTM-Gating*.

**5.2.3 Evaluation Metrics.** We exploit two frequently used metrics, namely RMSE (Root Mean Square Error) and MAE (Mean Absolute Error) to assess the performance of each method in each dataset. **RMSE** and **MAE** are computed by:

$$RMSE(y, \hat{y}) = \sqrt{\frac{1}{N} \sum_{i=1}^N (y_i - \hat{y}_i)^2}, MAE(y, \hat{y}) = \frac{1}{N} \sum_{i=1}^N |y_i - \hat{y}_i|$$

where  $y_i$  and  $\hat{y}_i$  are the ground truth and predict flows.

**avgNRMSE/avgNMAE** and **maxNRMSE/maxNMAE** are defined to assess the overall and the worst performance of each method. For convenience, we first give the definition of *NRMSE*. Suppose that there are a set of approach  $\mathcal{X}$  and several evaluation datasets  $\mathcal{D}$ , the *NRMSE* score of approach  $x(x \in \mathcal{X})$  in dataset  $d(d \in \mathcal{D})$  is

**Table 4: Early Jointly Modeling and Late Fusion Modeling results on different datasets. Every element represents the RMSE and the number of trainable parameters for each method (split by ’/’).**

	Bikesharing	Ridesharing	Metro	EV
	Chicago	Xi’an	Shanghai	Beijing
<i>STMeta</i>	2.740/489k	5.821/489k	<b>108.01/489k</b>	0.818/329k
<i>EarlyConcat</i>	3.294/896k	11.71/924k	574.31/924k	1.498/602k
<i>EarlyAdd</i>	2.701/489k	6.718/489k	184.53/489k	0.798/330k
<i>Raw-Concat</i>	2.665/491k	5.934/491k	130.73/491k	<b>0.783/332k</b>
<i>Raw-Add</i>	<b>2.632/493k</b>	<b>5.776/493k</b>	109.79/493k	0.935/334k

computed by:

$$\text{NRMSE}_{x,d} = \left( \frac{\text{RMSE}_{x,d}}{\min_{x' \in \mathcal{X}} (\text{RMSE}_{x',d})} \right)$$

The *avgNRMSE* metric is computed by averaging the *NRMSE* metrics in all datasets. Note that the more the *avgNRMSE* metric of one method is closer to 1, the better performance it has.

$$\text{avgNRMSE}_x = \text{Average}_{d \in \mathcal{D}} \left( \frac{\text{RMSE}_{x,d}}{\min_{x' \in \mathcal{X}} (\text{RMSE}_{x',d})} \right)$$

When applying maximum aggregation function to *NRMSE*, we will get *maxNRMSE* metric and it denotes the worst performance of an approach in all dataset.

$$\text{maxNRMSE}_x = \text{Maximum}_{d \in \mathcal{D}} \left( \frac{\text{RMSE}_{x,d}}{\min_{x' \in \mathcal{X}} (\text{RMSE}_{x',d})} \right)$$

We similarly define *avgNMAE* and *maxNMAE* metrics.

### 5.3 Modeling Techniques Impact on Prediction

Table 4 show the results on four scenarios by using *Concatenate* and *Add* variants of *Early Jointly Modeling* and *Late Fusion Modeling* techniques. From table 4, we observe that *Early Jointly Modeling* didn’t outperform *Late Fusion Modeling*, both in model accuracy and the number of trainable parameters, which is consistent with previous studies [27–29] that fusing cross-domain features in the high layer of neural network.

Table 5 show the results on seven datasets in four scenarios by using twelve variants of *Late Fusion Modeling*. From Table 5, we observe that modeling techniques are quite significant for leveraging useful information from context. Some variants (e.g. *Raw-Gating*) can extract extra useful context information which help to model crowd flow pattern and improve prediction accuracy in some datasets (e.g. *NYC* and *Chicago* datasets), yet it may also worsen original *STMeta* model performance in other datasets (e.g. *Chengdu*). This phenomenon actually suggests that context should be considered cautiously instead of indiscriminately fusing.

Precisely because choosing appropriate modeling techniques is exceedingly confusing, we give the following discussion.

**5.3.1 Late Fusion Modeling vs. Early Jointly Modeling.** In Table 4, it is obvious that *Early Jointly Modeling* (including *EarlyConcat* and *EarlyAdd*) is not better than the corresponding *Late Fusion Modeling*

techniques (including *Raw-Concat* and *Raw-Add*), both in model accuracy and the number of trainable parameters. *EarlyConcat* has larger trainable parameters than the others, but do not bring about an enhancement in accuracy. It is mainly because the spatiotemporal modeling units (namely *GCLSTM* [3]) can not capture context patterns from the perspective of space and time. *EarlyAdd* technique is better than *EarlyConcat* and have less trainable parameters but not so competitive as *Late Fusion Modeling*. The results in Table 4 shows that *Early Jointly Modeling* has not extracted more useful feature representations than *Late Fusion Modeling* but may cause higher computational complexity. Therefore, *Late Fusion Modeling* method is highly recommended.

**5.3.2 Embedding Layers Impact.** The *avgNRMSE* and *avgNMAE* metrics of the *MultiEmb* variants (contains multiple embedding layers, including *MultiEmb-Concat*, *MultiEmb-Add* and *MultiEmb-Gating*) are similar to *Emb* variants (contains single embedding layer, including *Emb-Concat*, *Emb-Add* and *Emb-Gating*) in Table 5. But the multiple embedding layers variants perform much worse than single embedding layer referencing to *maxNRMSE* and *maxNMAE* metrics. And it reveals that multiple embedding layers can not extract more context information beyond a single layer embedding layer but results in less generalization ability. In other words, stacking embedding layers can not make the model more robust. What’s more, the *avgNRMSE* and *avgNMAE* metrics of *Embedding* variants are worse compared with raw variants (e.g. *Raw-Gating*) and *LSTM* variants (e.g. *LSTM-Gating*), which suggests that handy embedding layer can not be acquired through end to end training.

**5.3.3 Historical Context Impact.** *LSTM* variants (including *LSTM-Concat*, *LSTM-Add* and *LSTM-Gating*) leverage *LSTM* to extract useful information from the past context in the fusion stage (Sec 4.2). Its *avgNRMSE/avgNMAE* and *maxNRMSE/maxNMAE* metrics are similar to *Raw* variants which suggests that the generality ability of these two variants are comparable. Expressly, the current context can provide enough extra information. It is worth mentioning that the above phenomena act at the setting of sixty minutes granularity. If the prediction interval is changed to smaller, the historical context may provide more information that helps predict the future flow.

**5.3.4 Fusion Method Impact.** *Concat*, *Add* and *Gating* are three choices to fuse context and other features in the fusion stage of *Late Fusion Modeling* (Sec 4.2). *Concat* variants preserves both original spatiotemporal and context features while *Add* variants fuse them by adding operator. Interestingly, these two variants perform similarly and worse than *Gating* variants in Table 5, which denotes that they have equivalent modeling capability. Moreover, *Raw-Gating* variant is remarkable and inspiring because it acquires lowest *avgNRMSE/avgNMAE* and *maxNRMSE/maxNMAE* compared to other variants especially to the *STMeta* model which do not incorporate any context feature. It shows *Raw-Gating*’s robustness and generalization ability applied to diverse application scenarios. Figure 2 shows the prediction results of two stations with the maximum flow in the Beijing electrical vehicle dataset. We see that *Raw-Gating* has a similar trend with *STMeta*, but *Raw-Gating* is closer to the ground truth at abnormal value (maximum flow and minimum flow, see the red circles 1~4 in Figure 2). This also fits our expectation: context features act as a switch that can help activate or flatten

**Table 5: 60-mins prediction results. RMSE/ MAE for each method. The best two results are highlighted in bold, and the top one result is further marked with “\*”.**

	Bikesharing		Ridesharing		Metro		EV	Overall	
	NYC	Chicago	Xi'an	Chengdu	Shanghai	Chongqing	Beijing	avgN[RMSE/MAE]	maxN[RMSE/MAE]
<i>STMeta</i>	3.605/2.251	2.740/1.571	5.821/3.696	<b>6.902*/4.294</b>	<b>154.5/70.48*</b>	92.84/50.68	0.818/0.461	1.047/1.034	1.100/1.074
<i>Raw-Concat</i>	<b>3.376/2.095*</b>	2.665/1.557	5.934/3.799	7.517/4.806	173.3/92.39	90.55/52.22	0.783/0.454	1.052/1.088	1.191/1.294
<i>Raw-Add</i>	3.405/2.117	2.632/1.549	<b>5.776*/3.699</b>	6.990/4.339	162.1/73.35	90.19/49.05	0.935/0.525	1.056/1.046	1.202/1.188
<i>Raw-Gating</i>	3.378/2.100	2.598/1.544	<b>5.801/3.656*</b>	<b>6.955/4.326</b>	<b>145.5*/71.38</b>	87.03/49.43	0.783/0.452	<b>1.009*/1.016*</b>	<b>1.032*/1.034*</b>
<i>Emb-Concat</i>	3.471/2.116	2.630/1.547	6.353/3.967	7.018/4.374	170.6/81.29	<b>84.37*/47.79*</b>	0.785/0.454	1.045/1.047	1.173/1.153
<i>Emb-Add</i>	3.413/2.120	2.701/1.523	5.968/3.734	7.038/4.416	162.6/83.84	87.38/49.77	<b>0.788/0.442*</b>	1.036/1.044	1.118/1.190
<i>Emb-Gating</i>	3.410/2.116	2.608/1.559	6.180/3.772	<b>6.956/4.264*</b>	193.2/86.69	<b>86.33/50.51</b>	0.787/0.447	1.058/1.053	1.328/1.230
<i>MultiEmb-Concat</i>	3.384/2.114	2.593/1.508*	5.829/3.716	7.367/4.842	179.6/95.10	<b>86.57/48.36</b>	0.793/0.450	1.047/1.077	1.234/1.349
<i>MultiEmb-Add</i>	3.452/2.146	2.634/1.540	6.061/3.912	7.320/4.823	175.7/99.74	91.14/50.32	<b>0.778*/0.444</b>	1.057/1.103	1.208/1.415
<i>MultiEmb-Gating</i>	3.392/2.102	2.690/1.562	6.132/3.786	7.033/4.353	231.9/106.7	89.34/50.02	<b>0.780/0.446</b>	1.099/1.095	1.594/1.514
<i>LSTM-Concat</i>	3.390/2.105	2.594/1.545	5.867/3.761	7.015/4.367	163.4/72.87	98.20/54.41	0.789/0.453	1.043/1.040	1.164/1.139
<i>LSTM-Add</i>	3.397/2.126	<b>2.580*/1.530</b>	5.980/3.770	7.006/4.326	162.8/78.35	93.66/51.78	0.787/0.454	1.039/1.042	1.119/1.112
<i>LSTM-Gating</i>	<b>3.367*/2.099</b>	<b>2.585/1.555</b>	6.020/3.726	7.000/4.309	156.4/71.45	90.48/50.64	0.784/0.449	<b>1.027/1.022</b>	<b>1.075/1.060</b>

the predicted value at an abnormal time. In general, *Raw-Gating* variants are robust modeling techniques with good generalization ability that help learn the anomalous crowd flow pattern with extra context information.

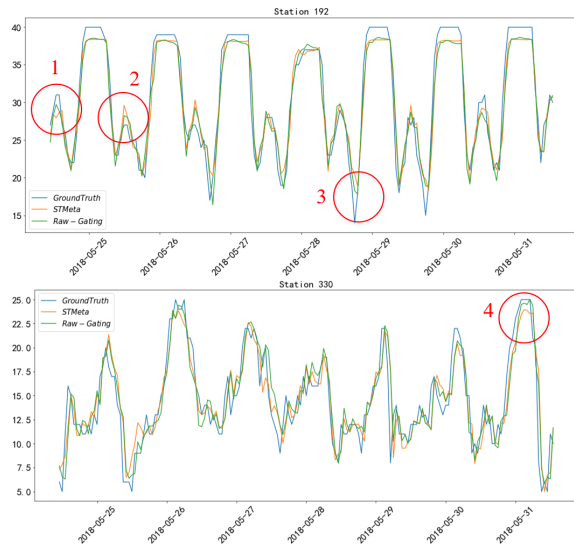


**Figure 2: Prediction results of two stations with the maximum flow in the Beijing electrical vehicle dataset. *Raw-Gating* variant is closer to the ground truth during low and peak hour.**

## 5.4 Context Features Impact on Prediction

To compare the generality ability of different kinds of context features, we design the ablation experiments by utilizing various combinations of context features. Table 6 shows the results of the above ablation experiments. Each row in Table 6 name as the context it contains. For example, *Raw-Gating-Wea-Holi* variant includes weather and holiday context. We choose *Raw-Gating* variant as the context modeling technique because it performs the best compared

to other modeling techniques in Table 5. Due to the inaccessibility of NYC, Chicago, Chongqing POI data, we do not conduct ablation experiments in these datasets.

**5.4.1 Data Distribution Imbalance Impact.** Intuitively, context features suffer from the data distribution imbalanced issue. For example, every season may have distinct weather characteristics and the data distribution of weather context is usually imbalanced. It snows only in winter, and it is hot in summer. As a result, when we use the weather data in summer to train STCFP models and predict the crowd flow in winter, the results may be bad since the weather context will not be generalized. Substantially, the imbalanced weather data will lead to less generalization ability which is further also confirmed by our experiments (Figure 3). We conduct experiments on different datasets that contain different time span of weather context based on the *STMeta* and *Raw-Gating*. The blue line in Figure 3 represents the results of *STMeta* which do not incorporates weather context. The blue line gradually converges when the number of training days is more than fifty days. The red line represents the result of *Raw-Gating* which incorporates weather data. The red line slowly converges when the number of training days is more than seventy-five days. From Figure 3, we observe that the *RMSE* metric of *Raw-Gating* (red line, with weather context) is a far cry from that of *STMeta* when the number of training days is less than thirty-one days, but gradually get close when the number of training days is more than seventy-five days. The *RMSE* metric of *Raw-Gating* is getting better because when the number of training days is correspondingly getting more, the weather distribution in the train set gradually covers the weather distribution in the test set.

That is to say, if we want to leverage context, we need to carefully check the distribution of context between train set and test set, especially when the time span of context is limited. This conclusion also is confirmed in Xi'an, Chengdu, and Shanghai datasets whose historical weather context only lasts for two or three months.

**5.4.2 Context Impact.** From Table 6, we see that the variants related to weather context like *STMeta-Wea* and *STMeta-Wea-Holi* have larger *avgNRMSE* and *avgNMAE* metrics which means that *weather* context is not as general as other context in Xi'an, Chengdu,

**Table 6: 60-mins ablation prediction results of different context features. The best two results are highlighted in bold, and the top one result is further marked with “\*”. RMSE/MAE for each method. (Wea: Weather; Holi: Holiday; TP: Temporal Position; POI: Point of Interest)**

	Bikesharing		Ridesharing		Metro		EV	Overall	
	NYC	Chicago	Xi'an	Chengdu	Shanghai	Chongqing	Beijing	avgN[RMSE/MAE]	maxN[RMSE/MAE]
<i>STMeta</i>	3.605/2.251	2.740/1.571	5.821/3.696	6.902/4.294	154.5/70.48	92.84/50.67	0.818/0.461	1.083/1.059	1.243/1.168
<i>Raw-Gating-Wea</i>	3.452/2.113	2.668/1.546	6.141/3.810	6.988/4.372	170.4/76.94	108.6/55.92	0.816/0.468	1.127/1.088	1.371/1.275
<i>Raw-Gating-Holi</i>	3.517/2.149	2.651/1.535	5.790/3.644	<b>6.841</b> */4.285	156.0/69.62	95.67/53.91	<b>0.782/0.442</b>	1.072/1.048	1.256/1.153
<i>Raw-Gating-TP</i>	3.409/ <b>2.094</b>	2.588/ <b>1.518</b>	5.685/3.612	6.967/4.261	131.7/ <b>61.14</b>	91.66/51.56	0.803/0.457	1.033/1.018	<b>1.079</b> /1.049
<i>Raw-Gating-POI</i>	-	-	5.821/3.683	6.912/4.310	149.3/67.46	-	0.798/0.444	1.069/1.043	1.202/1.118
<i>Raw-Gating-Wea-Holi</i>	3.455/2.150	2.652/1.549	6.064/3.785	6.894/4.284	164.3/77.53	101.0/56.08	0.800/0.453	1.100/1.083	1.323/1.284
<i>Raw-Gating-Wea-TP</i>	<b>3.361</b> */ <b>2.089</b> *	<b>2.553</b> */ <b>1.503</b> *	5.941/3.702	6.967/4.317	143.6/71.21	<b>84.95</b> */ <b>49.14</b> *	<b>0.780/0.442</b>	1.034/1.034	1.156/1.180
<i>Raw-Gating-Wea-POI</i>	-	-	6.396/3.914	7.271/4.615	185.9/84.98	-	0.820/0.468	1.189/1.164	1.496/1.408
<i>Raw-Gating-Holi-TP</i>	3.410/2.126	<b>2.554</b> / <b>1.503</b> *	5.699/3.630	6.929/4.272	<b>124.2</b> */ <b>60.36</b> *	93.69/52.03	<b>0.779</b> */ <b>0.439</b> *	<b>1.021</b> / <b>1.014</b>	1.103/1.059
<i>Raw-Gating-Holi-POI</i>	-	-	5.761/3.646	<b>6.858</b> / <b>4.256</b> *	159.0/67.82	-	<b>0.783/0.442</b>	1.079/1.038	1.280/1.124
<i>Raw-Gating-TP-POI</i>	-	-	<b>5.593</b> */ <b>3.572</b> *	6.895/4.279	137.0/62.24	-	0.787/0.444	1.030/ <b>1.012</b> *	1.103/ <b>1.031</b> *
<i>Raw-Gating-Wea-Holi-TP</i>	<b>3.378</b> /2.100	2.598/1.544	5.801/3.656	6.955/4.326	145.5/71.38	<b>87.03</b> / <b>49.43</b>	0.783/0.452	1.040/1.042	1.171/1.183
<i>Raw-Gating-Wea-Holi-POI</i>	-	-	6.072/3.756	7.078/4.575	171.6/82.06	-	0.805/0.460	1.134/1.133	1.381/1.359
<i>Raw-Gating-Wea-TP-POI</i>	-	-	6.042/3.783	6.950/4.387	171.3/84.77	-	0.789/0.458	1.122/1.134	1.379/1.404
<i>Raw-Gating-Holi-TP-POI</i>	-	-	<b>5.654</b> / <b>3.607</b>	6.870/4.257	<b>131.4</b> /62.48	-	<b>0.779</b> */ <b>0.445</b>	<b>1.018</b> */1.015	<b>1.058</b> */ <b>1.035</b>
<i>Raw-Gating-All</i>	-	-	5.835/3.663	6.955/4.419	154.9/72.47	-	0.781/0.452	1.077/1.073	1.247/1.201

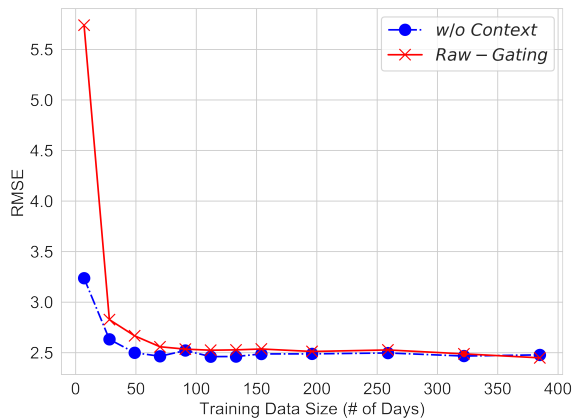


**Figure 3: The RMSE metric of different training data size which represents different distributions of weather context) experiments. The experiments are conducted on Chicago dataset.**

Shanghai and Chongqing datasets. On the contrary, the variants that contain *Temporal Position* context (including *Raw-Gating-Holi-TP* and *Raw-Gating-TP-POI*) outperform that of other kinds of context. This suggests that *temporal position* context is more likely useful to provide extra information that helps *STMeta* model better capture crowd flow pattern. To verify the generality ability of different kinds of context, we give the rank of the above four types of context based on the *avgNRMSE/avgNMAE* and *maxNRMSE/maxNMAE* metrics of *Raw-Gating-Wea*, *Raw-Gating-Holi*, *Raw-Gating-TP*, and *Raw-Gating-POI* variants in Table 6.

*Temporal Position* > *POI* > *Holiday* > *Weather*

Interestingly enough, previous research [19] says that the more knowledge, the better prediction, and we do not observe similar phenomena based on our experiments which reveals that existing

modeling techniques may not be robust enough to capture patterns from all kinds of context.

## 5.5 Guidelines and Insights

Based on our large-scale analytical and experimental empirical study, we summarize several guidelines for the follow-up researchers to conveniently make full use of context in diverse applications.

**Context Guideline:** Context including *weather*, *holiday*, *temporal position*, and *POI* could be considered in almost all kind of STCFP scenarios, but with different generalization ability. *Temporal Position*, *Holiday*, and *POI* have better generalization ability than *Weather* which inspires us to pay more attention. Additionally, *Temporal Position* and *Holiday* context data is cheaper to access and thus are prior recommended.

**Modeling Techniques Guideline:** *Late Fusion Modeling* is more competitive than *Early Jointly Modeling* both in computational complexity and model capabilities. That is to say, fusing context in the high-level layer of the neural network is a better choice rather than in the low-level layer. Besides, in *Late Fusion Modeling* branch, *Raw-Gating* is highly recommended because it performs the best in almost every scenario which verifies its great generalization ability. Moreover, *Raw-Gating* technique doesn’t need to tune fusing parameters and bring few computational burdens.

**Data Distribution Insight:** The data distribution imbalance issue of context between test set and train set may result in worse prediction result compared to the models without context. The data distribution imbalance issue may relieve if more context data acquired. It reminds us that we should carefully check the distribution of context before leveraging context.

## 6 RELATED WORK

### 6.1 Time Series Prediction

Earlier research regarded the crowd flow prediction as a classic time series prediction problem. Hamed [7] applied the Autoregressive Integrated Moving Average (ARIMA) to forecast short-term traffic on the highway. ARIMA is a linear model that assumes that future



crowd flow is related to historical observation. But this assumption is not consistent with the actual crowd flow characteristics. Many nonlinear algorithms such as support vector machine [5], Markov random field [8], decision tree method [11] and bayesian network [18] model the temporal dependencies very well, yet it fails to capture spatial correlations and leverage context information.

## 6.2 Spatio-Temporal Prediction

With the enhancement of computing performance and the development of deep learning technology, Convolutional Neural Network (CNN) and Graph Convolutional Network (GCN) are used to model spatial dependency in crowd flow prediction problems. Zhang et al. [27] split the city traffic flow into grids according to time order, and then use CNN to capture the spatial dependency. Ke et al. [9] used convolution long-short term memory network (Conv-LSTM) to simultaneously capture the spatiotemporal dependencies of taxi demand. Geng et al [6] use a multi-graph convolution model to capture varieties of spatial knowledge. However, whereas these previous studies attempt to make full use of spatiotemporal correlations, the focus of this work is exploring the generality of both context and its modeling techniques.

## 7 CONCLUSION

In this paper, we focus on exploring the generalization ability of both context and its modeling techniques in the classic STCFP problem which is also inspiring to other questions. We conduct a large-scale analytical and experimental empirical study. In the analytical study, we investigate general context features and classify them into four categories: weather, holiday, temporal position, and POI. We further give a taxonomy on existing context modeling techniques. Based on the above analytical study, we conduct large-scale experiments on seven real-world datasets to verify the generalization ability of both general context and context modeling techniques in different STCFP application scenarios. Eventually, we give some guidelines for the researchers that need to incorporate the context into their application scenarios based on our analysis and insights.

## REFERENCES

- [1] Gregory D Abowd, Anind K Dey, Peter J Brown, Nigel Davies, Mark Smith, and Pete Steggle. 1999. Towards a better understanding of context and context-awareness. In *International symposium on handheld and ubiquitous computing*. 304–307.
- [2] Sungwoo Bae and Alexis Kwasinski. 2011. Spatial and temporal model of electric vehicle charging demand. *IEEE Transactions on Smart Grid* 3, 1 (2011), 394–403.
- [3] Di Chai, Leye Wang, and Qiang Yang. 2018. Bike Flow Prediction with Multi-Graph Convolutional Networks. In *Proceedings of the 26th ACM SIGSPATIAL International Conference on Advances in Geographic Information Systems*. 397–400.
- [4] K. Chen, F. Chen, B. Lai, Z. Jin, Y. Liu, K. Li, L. Wei, P. Wang, Y. Tang, J. Huang, and X. S. Hua. 2020. Dynamic Spatio-Temporal Graph-Based CNNs for Traffic Flow Prediction. *IEEE Access* 8 (2020), 185136–185145.
- [5] Yuliang Cong, Jianwei Wang, and Xiaolei Li. 2016. Traffic flow forecasting by a least squares support vector machine with a fruit fly optimization algorithm. *Procedia Engineering* 137, 1 (2016), 59–68.
- [6] Xu Geng, Yaguang Li, Leye Wang, Lingyu Zhang, Qiang Yang, Jieping Ye, and Yan Liu. 2019. Spatiotemporal multi-graph convolution network for ride-hailing demand forecasting. In *AAAI*, Vol. 33. 3656–3663.
- [7] Mohammad M. Hamed, Hashem R. Al-Masaied, and Zahi M. Bani Said. 1995. Short-Term Prediction of Traffic Volume in Urban Arterials. *Journal of Transportation Engineering* 121, 3 (1995), 249–254.
- [8] Minh X. Hoang, Yu Zheng, and Ambuj K. Singh. 2016. FCCF: Forecasting Citywide Crowd Flows Based on Big Data. In *Proceedings of the 24th ACM SIGSPATIAL International Conference on Advances in Geographic Information Systems*. Article 6, 10 pages.
- [9] Jintao Ke, Hongyu Zheng, Hai Yang, and Xiqun (Michael) Chen. 2017. Short-term forecasting of passenger demand under on-demand ride services: A spatio-temporal deep learning approach. *Transportation Research Part C: Emerging Technologies* 85 (2017), 591–608.
- [10] Yaguang Li, Rose Yu, Cyrus Shahabi, and Yan Liu. 2018. Diffusion Convolutional Recurrent Neural Network: Data-Driven Traffic Forecasting. In *International Conference on Learning Representations (ICLR '18)*.
- [11] Yexin Li, Yu Zheng, Huichu Zhang, and Lei Chen. 2015. Traffic prediction in a bike-sharing system. In *Proceedings of the 23rd SIGSPATIAL International Conference on Advances in Geographic Information Systems - GIS '15*. 1–10.
- [12] Yuxuan Liang, Songyu Ke, Junbo Zhang, Xiuwen Yi, and Yu Zheng. 2018. Geo-MAN: Multi-level Attention Networks for Geo-sensory Time Series Prediction. In *Proceedings of the Twenty-Seventh International Joint Conference on Artificial Intelligence*. 3428–3434.
- [13] Ziqian Lin, Jie Feng, Ziyang Lu, Yong Li, and Depeng Jin. 2019. DeepSTN+: Context-Aware Spatial-Temporal Neural Network for Crowd Flow Prediction in Metropolis. In *AAAI*, Vol. 33. 1020–1027.
- [14] Yang Liu, Zhiyuan Liu, and Ruo Jia. 2019. DeepPF: A deep learning based architecture for metro passenger flow prediction. *Transportation Research Part C: Emerging Technologies* 101 (2019), 18–34.
- [15] Yongxin Tong, Yuqiang Chen, Zimu Zhou, Lei Chen, Jie Wang, Qiang Yang, Jieping Ye, and Weifeng Lv. 2017. The Simpler The Better: A Unified Approach to Predicting Original Taxi Demands based on Large-Scale Online Platforms. In *Proceedings of the 23rd ACM SIGKDD International Conference on Knowledge Discovery and Data Mining - KDD '17*. 1653–1662.
- [16] Petar Veličković, Guillem Cucurull, Arantxa Casanova, Adriana Romero, Pietro Liò, and Yoshua Bengio. 2018. Graph attention networks. *International Conference on Learning Representations* (2018).
- [17] Dong Wang, Wei Cao, Jian Li, and Jieping Ye. 2017. DeepSD: Supply-Demand Prediction for Online Car-Hailing Services Using Deep Neural Networks. In *2017 IEEE 33rd International Conference on Data Engineering (ICDE)*. 243–254.
- [18] Jian Wang, Wei Deng, and Yuntao Guo. 2014. New Bayesian combination method for short-term traffic flow forecasting. *Transportation Research Part C: Emerging Technologies* 43 (2014), 79–94.
- [19] Leye Wang, Di Chai, Xuanchu Liu, Liyue Chen, and Kai Chen. 2020. Exploring the Generalizability of Spatio-Temporal Crowd Flow Prediction: Meta-Modeling and an Analytic Framework. *arXiv preprint arXiv:2009.09379* (2020).
- [20] Yu Wei and Mu-Chen Chen. 2012. Forecasting the short-term metro passenger flow with empirical mode decomposition and neural networks. *Transportation Research Part C: Emerging Technologies* 21, 1 (2012), 148–162.
- [21] Fei Wu, Hongjian Wang, and Zhenhui Li. 2016. Interpreting Traffic Dynamics Using Ubiquitous Urban Data. In *Proceedings of the 24th ACM SIGSPATIAL International Conference on Advances in Geographic Information Systems*. Article 69, 4 pages.
- [22] Zidong Yang, Ji Hu, Yuanchao Shu, Peng Cheng, Jiming Chen, and Thomas Moscibroda. 2016. Mobility Modeling and Prediction in Bike-Sharing Systems. In *Proceedings of the 14th Annual International Conference on Mobile Systems, Applications, and Services - MobiSys '16*. 165–178.
- [23] Huaxiu Yao, Xianfeng Tang, H. Wei, Guanjie Zheng, Y. Yu, and Z. Li. 2018. Modeling Spatial-Temporal Dynamics for Traffic Prediction. *ArXiv abs/1803.01254* (2018).
- [24] Huaxiu Yao, F. Wu, Jintao Ke, Xianfeng Tang, Yitian Jia, Siyu Lu, Pinghua Gong, Jieping Ye, and Z. Li. 2018. Deep Multi-View Spatial-Temporal Network for Taxi Demand Prediction. In *AAAI 2018*. 2588–2595.
- [25] Xiuwen Yi, Zhewen Duan, Ting Li, Tianrui Li, Junbo Zhang, and Yu Zheng. 2019. Citytraffic: Modeling citywide traffic via neural memorization and generalization approach. In *Proceedings of the 28th ACM International Conference on Information and Knowledge Management*. 2665–2671.
- [26] Nicholas Jing Yuan, Yu Zheng, Xing Xie, Yingzi Wang, Kai Zheng, and Hui Xiong. 2014. Discovering urban functional zones using latent activity trajectories. *IEEE Transactions on Knowledge and Data Engineering* 27, 3 (2014), 712–725.
- [27] Junbo Zhang, Yu Zheng, and Dekang Qi. 2017. Deep Spatio-Temporal Residual Networks for Citywide Crowd Flows Prediction. In *Proceedings of the Thirty-First AAAI Conference on Artificial Intelligence*. 1655–1661.
- [28] Junbo Zhang, Yu Zheng, Dekang Qi, Ruiyuan Li, and Xiuwen Yi. 2016. DNN-based prediction model for spatio-temporal data. In *Proceedings of the 24th ACM SIGSPATIAL International Conference on Advances in Geographic Information Systems*. 1–4.
- [29] Junbo Zhang, Yu Zheng, Junkai Sun, and Dekang Qi. 2019. Flow Prediction in Spatio-Temporal Networks Based on Multitask Deep Learning. *IEEE Transactions on Knowledge and Data Engineering* (2019), 1–1.
- [30] L. Zhu and N. Laptev. 2017. Deep and Confident Prediction for Time Series at Uber. In *2017 IEEE International Conference on Data Mining Workshops (ICDMW)*. 103–110.

- [31] Ali Zonoozi, Jung jae Kim, Xiao-Li Li, and Gao Cong. 2018. Periodic-CRN: A Convolutional Recurrent Model for Crowd Density Prediction with Recurring Periodic Patterns. In *Proceedings of the Twenty-Seventh International Joint Conference on Artificial Intelligence, IJCAI-18*. 3732–3738.

## A WEATHER CONTEXT RESOURCES

Holiday and temporal context can be effortlessly acquired by the official calendar provided by the government. However, weather context is hard to collect. Therefore, we summarize some weather context resources in Table A1.

## B EXPERIMENT HYPERPARAMETERS

STMeta is our backbone network and we choose GCLSTM [3] as spatiotemporal modeling unit and GAL [16] as spatiotemporal aggregation unit. The hidden states and the number of multi-head in GCLSTM are 64 and 2. The output dimensions of the embedding layer (related to *Emb* and *MultiEmb* variants) are also critical in the context representation stage. We use Microsoft NNI<sup>3</sup> package to find out the best output dimensions in each dataset. The output dimensions of *Emb* and *MultiEmb* variants are 10 and 10-1-6 (corresponding to weather, holiday, and temporal position context).

## C DATA DESCRIPTION

### C.1 Bikesharing

The bikesharing dataset is collected from U.S. open data portals including New York City<sup>4</sup> and Chicago<sup>5</sup>. The time span of this dataset is more than one year and each piece of valid record contains the start station, start time, stop station, stop time, etc. We predict the number of bikesharing demands in each station at the next moment.

### C.2 Ridesharing

The ridesharing dataset is collected from DiDi's open research project<sup>6</sup>. This dataset contains ridesharing orders in Chinese cities Xi'an and Chengdu for two months. Each record contains start location, start time, end location, and end time. The location information has longitude and latitude. We respectively split the central area of two cities into  $16 \times 16$  grids with a size of  $0.5km \times 0.5km$  for each grid, then we predict the number of taxi orders in each grid.

### C.3 Metro

The metro dataset contains metro trip records in Shanghai and Chongqing. The time span of Shanghai and Chongqing are three months and one year respectively. Each metro trip record has the check-in time, check-in station, check-out time, and check-out station. We predict the check-in flow amount for all the metro stations.

### C.4 Electrical Vehicle (EV)

The electrical vehicle (EV) dataset is collected from Beijing whose period is six months. This dataset contains the occupation situation

at different time slots. Each record contains sensing time, available and occupied docks. We predict the number of docks in use at the next moment for each station as it is the most important demand indicator of the charging stations.

## C.5 Context Features

We collect weather data from the OpenWeatherMap website<sup>7</sup> and its original granularity is 60-minutes. We regard the weather data measured by one meteorological station in each city as the weather data of the entire city. For the holiday context data, we parse holiday information by using *chinese\_calendar*<sup>8</sup> and *workalendar* package<sup>9</sup>. For the temporal position features, we transform *DayofWeek* and *HourofDay* features by using one-hot encoding as mentioned in Sec 3.1.3. POI data is crawled from the online map<sup>10</sup>.

## D DATA AND CODE

We have released the data and code for reproducing our experiment results at <https://anonymous.4open.science/r/0a04c2cc-028d-4e39-b52d-84f5688d62fb/> for the blind review.

<sup>3</sup><https://github.com/microsoft/nni>

<sup>4</sup><https://www.citibikenyc.com/system-data>

<sup>5</sup><https://www.divvybikes.com/system-data>

<sup>6</sup><https://outreach.didichuxing.com/app-vue/TTItrajectory?id=1001>

<sup>7</sup><https://openweathermap.org/history-bulk>

<sup>8</sup><https://pypi.org/project/chinesecalendar/0.0.4/>

<sup>9</sup><https://github.com/peopledoc/workalendar>

<sup>10</sup><https://map.baidu.com/>

**Table A1: Weather context resources**

Resources Description	Temporal Granularity	Link
American weather and climate data	15/60-mins	<a href="https://www.ncdc.noaa.gov/cdo-web/">https://www.ncdc.noaa.gov/cdo-web/</a>
Shanghai historical weather and climate data	10-mins	<a href="http://soda.data.sh.gov.cn/competitionData.html">http://soda.data.sh.gov.cn/competitionData.html</a>
Glovable real-time and historical Weather data	5/60-mins	<a href="https://www.wunderground.com/">https://www.wunderground.com/</a>
Global weather and climate data	60-mins	<a href="https://openweathermap.org/">https://openweathermap.org/</a>
Australia climate data and services	daily	<a href="http://www.bom.gov.au/climate/data/">http://www.bom.gov.au/climate/data/</a>
Canada historical climate data	60-mins	<a href="https://climate.weather.gc.ca/">https://climate.weather.gc.ca/</a>
Global climate data records from the surface and troposphere	daily	<a href="https://cds.climate.copernicus.eu/">https://cds.climate.copernicus.eu/</a>

**Table C1: Dataset statistics**

	Bikesharing		Ridesharing		Metro		EV
	NYC	Chicago	Xi'an	Chengdu	Shanghai	Chongqing	Beijing
<b>Time Span</b>	2013.03-2014.09	2013.07-2014.09	2016.10-2016.11	2016.10-2016.11	2016.07-2016.09	2016.08-2017.07	2018.03-2018.05
# Locations	820	585	256	256	288	113	629
Weather Granularity	60-mins	60-mins	60-mins	60-mins	60-mins	60-mins	60-mins
# Holiday	3624	3624	240	240	298	1924	312